Journal of Hydraulic Research

ISSN: 0022-1686 (Print) 1814-2079 (Online) Journal homepage: http://www.tandfonline.com/loi/tjhr20

Variable Shields number model for river bankfull geometry: bankfull shear velocity is viscosity-dependent but grain size-independent

Chuan Li, Matthew J. Czapiga, Esther C. Eke, Enrica Viparelli & Gary Parker

To cite this article: Chuan Li, Matthew J. Czapiga, Esther C. Eke, Enrica Viparelli & Gary Parker (2015) Variable Shields number model for river bankfull geometry: bankfull shear velocity is viscosity-dependent but grain size-independent, Journal of Hydraulic Research, 53:1, 36-48, DOI: 10.1080/00221686.2014.939113

To link to this article: http://dx.doi.org/10.1080/00221686.2014.939113

IAHR AIRH
Taylor & Francis
Taylor & Francis Group

Journal of Hydraulic Research Vol. 53, No. 1 (2015), pp. 36–48
http://dx.doi.org/10.1080/00221686.2014.939113

Research paper

Variable Shields number model for river bankfull geometry: bankfull shear velocity is viscosity-dependent but grain size-independent

CHUAN LI, Graduate Research Assistant, *Ven Te Chow Hydrosystems Laboratory, Department of Civil and Environmental Engineering, University of Illinois at Urbana-Champaign, Urbana, IL, USA*
Email: chuanli2@illinois.edu (author for correspondence)

MATTHEW J. CZAPIGA (IAHR Member), Graduate Research Assistant, *Ven Te Chow Hydrosystems Laboratory, Department of Civil and Environmental Engineering, University of Illinois at Urbana-Champaign, Urbana, IL, USA*
Email: czapiga2@illinois.edu

ESTHER C. EKE (IAHR Member), Postdoctoral Research Associate, *Department of Geography and Environmental Engineering, Johns Hopkins University, Baltimore, MD, USA*
Email: eeke1@jhu.edu

ENRICA VIPARELLI (IAHR Member), Assistant Professor, *Department of Civil and Environmental Engineering, University of South Carolina, Columbia, SC, USA*
Email: viparell@cec.sc.edu

GARY PARKER (IAHR Member), Professor, *Ven Te Chow Hydrosystems Laboratory, Department of Civil and Environmental Engineering and Department of Geology, University of Illinois at Urbana-Champaign, Urbana, IL, USA*
Email: parkerg@illinois.edu

ABSTRACT
The bankfull geometry of alluvial rivers is thought to be controlled by water and sediment supply, and characteristic sediment size. Here we demonstrate a novel finding: when bankfull shear velocity and bankfull depth are correlated against bed material grain size and bed slope, they are to first order independent of grain size and dependent on water viscosity. We demonstrate this using a similarity collapse for bankfull Shields number as a function of slope and grain size, obtained with data for 230 river reaches ranging from silt-bed to cobble-bed. Our analysis shows that bankfull Shields number increases with slope to about the half power. We show that the new relation for bankfull Shields number provides more realistic predictions for the downstream variation of bankfull characteristics of rivers than a previously used assumption of constant bankfull Shields number.

Keywords: River bankfull geometry; Shields number

1 Introduction

The bankfull geometry of alluvial rivers is characterized in terms of bankfull width B_{bf}, bankfull depth H_{bf} and bankfull discharge Q_{bf} (Leopold and Maddock 1953). The physics behind these relations also involves characteristic bed material grain size D, submerged specific gravity of sediment R (∼1.65 for quartz), water viscosity ν, bed slope S and total volume bed material load (bedload plus suspended bed material load) Q_{tbf} at bankfull flow (Parker *et al.* 2007, Wilkerson and Parker 2011).

A central question of river hydraulics is how channel characteristics vary with flood discharge, sediment supply and sediment size. The problem can be characterized in terms of relations for B_{bf}, H_{bf} and S as functions of Q_{bf}, Q_{tbf} and D. Earlier attempts to specify closures for these relations have assumed a specified formative (bankfull) channel Shields number τ^*_{bf} (Paola *et al.*

Received 17 February 2014; accepted 16 June 2014/Currently open for discussion.

ISSN 0022-1686 print/ISSN 1814-2079 online
http://www.tandfonline.com

1992, Parker *et al.* 1998a, 1998b). The bankfull Shields number is useful as part of a closure scheme for bankfull geometry because it provides, under the approximation of steady, uniform flow, a relation for the product of bankfull depth and bed slope. Based on earlier work of Parker (1978), Paola *et al.* (1992) first used the assumption of constant bankfull Shields number to study the response of a gravel-bed river profile to subsidence. The corresponding assumption for sand-bed rivers, but with a much higher bankfull Shields number, has been implemented by Parker *et al.* (1998a, 1998b). With a relatively sparse data set, Parker *et al.* (1998a, 1998b) found that the bankfull Shields number in alluvial streams could be crudely approximated invariant to other characteristics of rivers, e.g. bed slope. The constant values 0.042 (Parker *et al.* 1998a) or 0.049 (Parker 2004) have been suggested for gravel-bed rivers, and the constant values 1.8 (Parker *et al.* 1998b) or 1.86 (Parker 2004, Parker *et al.* 2008) have been used for sand-bed rivers. These authors used the assumption of a constant formative Shields number, combined with momentum balance, continuity relations for water and bed material load, and bed material sediment transport equations, to develop predictive relations for bankfull width, bankfull depth and bed slope as functions of bankfull discharge and bed material transport at bankfull flow. The resulting relations have been applied to study how rivers respond to basin subsidence and rising base level (Paola *et al.* 1992, Parker *et al.* 1998b, Parker 2004) and how deltas evolve (Kim *et al.* 2009).

Here we rely on three compendiums of data on bankfull characteristics of single-thread alluvial channels to revisit the empirical formulation for bankfull Shields number (Parker *et al.* 2007, Wilkerson and Parker 2011, Latrubesse, personal communication). The data base includes 230 river reaches, with Q_{bf} varying from 0.34 to 216,340 m^3s^{-1}, B_{bf} varying from 2.3 to 3400 m, H_{bf} varying from 0.22 to 48.1 m, S varying from 8.8×10^{-6} to 5.2×10^{-2}, and D varying from 0.04 to 168 mm. One reach from the original data was omitted as the representative grain size was much finer than the other reaches.

The data used in Parker *et al.* (2007) pertain to rivers for which $D \geq 25$ mm. They were obtained from four sources, the references for which are documented in the original paper on page 3 and the list of references. The data used in Wilkerson *et al.* (2011) pertain to rivers for which $D < 25$ mm. They were obtained from 26 sources, the references for which are documented in Table 1 in the original paper and the list of references. The data from Latrubesse (personal communication) pertain to tropical sand-bed rivers, most of them very large (i.e. bankfull discharge $\geq 20,000\ m^3s^{-1}$). These data were screened in detail to determine suitability for analysis. For example, the large data set of Soar and Thorne (2001) was excluded because bankfull discharge was computed rather than measured. The entire data set used in this study can be downloaded from the site: http://hydrolab.illinois.edu/people/parkerg//VariableShieldsModelBasicData.htm.

2 Formulation of the new relation for bankfull Shields number

We estimate bankfull boundary shear stress τ_{bf} using the normal flow approximation for momentum balance:

$$\tau_{bf} = \rho g H_{bf} S \tag{1}$$

where ρ is water density and g is gravitational acceleration. The dimensionless Shields number is

$$\tau^*_{bf} = \frac{\tau_{bf}}{\rho R g D} \tag{2}$$

Here $R = 1.65$ is the submerged specific gravity for quartz. Between Eqs. (1) and (2),

$$\tau^*_{bf} = \frac{H_{bf} S}{R D} \tag{3}$$

We define dimensionless grain size D^* as (van Rijn 1984)

$$D^* = \frac{(Rg)^{1/3}}{\nu^{2/3}} D \tag{4}$$

where ν denotes the kinematic viscosity of water. In all the calculations here, ν is assumed to take the value $1 \times 10^{-6}\ m^2s^{-1}$ in the absence of direct measurements. It is worth noting, however, that for water, ν varies only from 1.52×10^{-6} to $0.80 \times 10^{-6}\ m^2s^{-1}$ as temperature varies from 5 to 30 °C.

Figure 1a shows a plot of τ^*_{bf} versus D^* in the form of a Shields diagram (Parker *et al.* 2008), with lines indicating the approximate inception of bedload transport and the approximate initiation of significant suspension. The data have been stratified into five grain size ranges: 0.04–0.062 mm (silt), 0.062–0.5 mm (very fine to medium sand), 0.5–2 mm (coarse to very coarse sand), 2–25 mm (fine to coarse gravel) and 25–168 mm (coarse gravel to cobbles). The data cover the range from suspended load-dominated rivers to bedload-dominated rivers. The figure shows a consistent trend, with τ^*_{bf} decreasing with increasing D^*, that has been noted earlier by Dade and Friend (1998).

Figure 1b shows a corresponding plot of τ^*_{bf} versus bed slope S, with the same grain size discrimination: it is seen that τ^*_{bf} is an increasing function of S through every grain size range. While a tendency for critical Shields number (corresponding to the onset of motion) to increase with S has been reported previously (Lamb *et al.* 2008, Recking 2009), here we demonstrate this tendency for bankfull Shields number as well. This tendency was first noted for a data set corresponding to D ranging from 17 to 36 mm (Mueller and Pitlick 2005) here we demonstrate it over D ranging from 0.04 to 168 mm.

Figure 1 suggests the use of similarity collapse to obtain a universal relation for τ^*_{bf} as a function of S and D^*. We performed the analysis by seeking an exponent m in the relation $\tau^*_{bf} \sim S^m$, applicable to all grain sizes, and then performing a power regression analysis of τ^*_{bf}/S^m versus D^*. The relation so obtained is

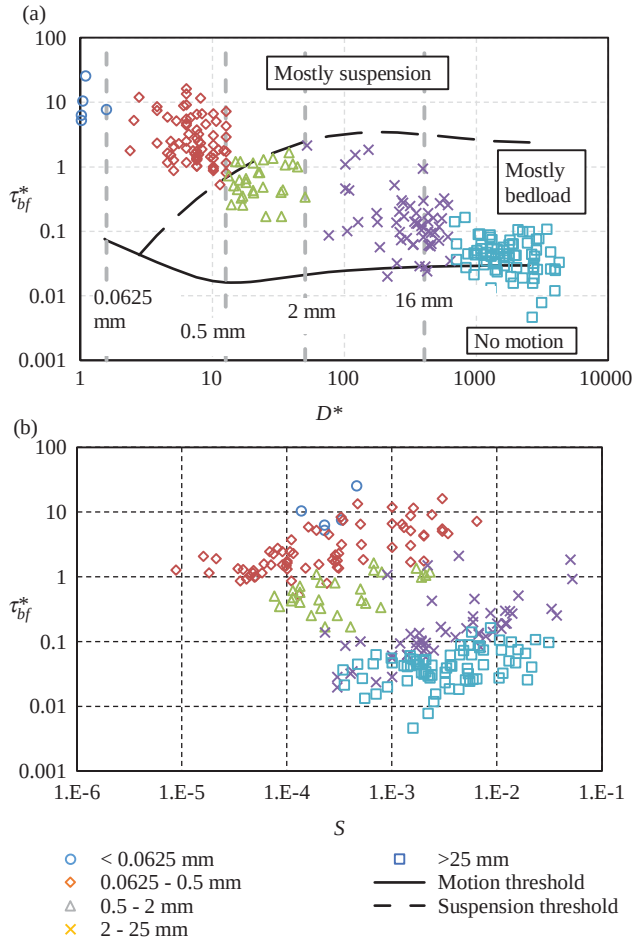

Figure 1 Bankfull Shields number τ^*_{bf} versus (a) dimensionless grain size D^* and (b) bed slope S for rivers ranging from silt-bed to cobble-bed. The data are stratified into five grain size ranges. Note that τ^*_{bf} increases with slope for every grain size range. Also shown in (a) are lines denoting the onset of bed motion and the onset of significant sediment suspension

$\tau^*_{bf} = 1223(D^*)^{-1.00}S^{0.534}$, with a coefficient of determination $R^2 = 0.948$, as shown in Fig. 2. Rounding appropriately,

$$\tau^*_{bf} = \beta \left(D^*\right)^{-1} S^m \tag{5}$$

where $\beta = 1220$ and $m = 0.53$.

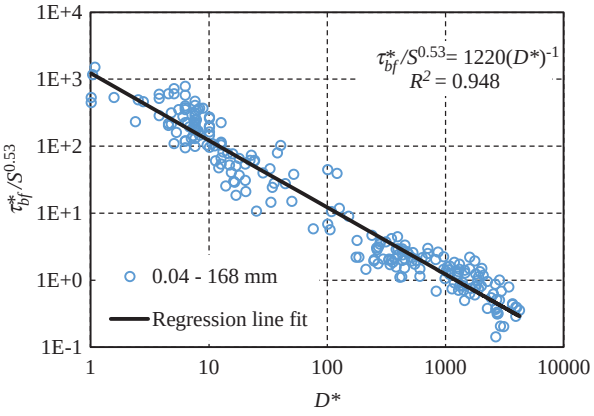

Figure 2 Similarity collapse for $\tau^*_{bf}/S^{0.53}$ versus D^*. The regression relation, i.e. Eq. (5), is shown in the plot

The conclusion in Eq. (5) that the exponent of D^* is -1.00 is confirmed by splitting the data into two subsets, one for which $D \leq 25$ mm and one for which $D > 25$ mm. The corresponding exponents of D^* are -0.096 and -1.048, i.e only a very modest deviation from -1.00. It is seen from Eq. (4) that D^* depends on $\nu^{-2/3}$. As noted above, ν has been set equal to 1×10^{-6} m^{2}s^{-1}, i.e. the standard value for water. In order to study the effect of varying ν, this parameter was randomized between the values 0.80×10^{-6} m^{2}s^{-1} (30 °C) and 1.52×10^{-6} m^{2}s^{-1} (5 °C). The randomization was different for each river reach. Ten implementations of this randomization yielded exponents ranging from -0.9904 to -1.0004.

3 Implications for bankfull shear velocity and depth

The value of the exponent of D^* in Eq. (5), i.e. -1, has an unexpected consequence. The definition for τ^*_{bf} of Eq. (2) is such that it varies as D^{-1}, but the right-hand side of Eq. (5) also varies as D^{-1}. Defining bankfull shear velocity u_{*bf} as

$$u_{*bf} = \left(\frac{\tau_{bf}}{\rho}\right)^{1/2} \tag{6}$$

it follows that bed material grain size precisely cancels out in the relation for bankfull shear velocity from Eqs. (2), (5) and (6). With the aid of Eq. (5), Eq. (3) can be solved for H_{bf}; and the bed material grain size again cancels out in the relation for bankfull water depth.

The present analysis thus yields a remarkable, and indeed counterintuitive result: bankfull shear velocity and bankfull depth do not depend on the characteristic grain size of the bed material, as shown by the resulting dimensionless relations,

$$\tilde{u}_{*bf} = 35.0S^{0.26} \tag{7a}$$

$$\tilde{H}_{bf} = 1220\,S^{-0.47} \tag{7b}$$

where the dimensionless shear velocity $\tilde{u}_{*bf}$ and depth $\tilde{H}_{bf}$ are

$$\tilde{u}_{*bf} = \frac{u_{*bf}}{(Rg\nu)^{1/3}} \tag{8a}$$

$$\tilde{H}_{bf} = \frac{H_{bf}g^{1/3}}{(R\nu)^{2/3}} \tag{8b}$$

Equations (7a) and (7b), which are compared against the original data set in Figs. 3a and 3b, are of a curious form. Firstly, they specify bankfull shear velocity and bankfull depth independent of characteristic bed grain size across the entire grain size range studied here (0.04–168 mm). Secondly, they show a dependence on kinematic viscosity across the same grain size range, and across the entire range of flow discharges (0.34–216,000 m^{3}s^{-1}).

In so far as Eqs. (2) and (5) both depend upon D^{-1}, the absence of grain size dependence in Eq. (7a) and (7b) might

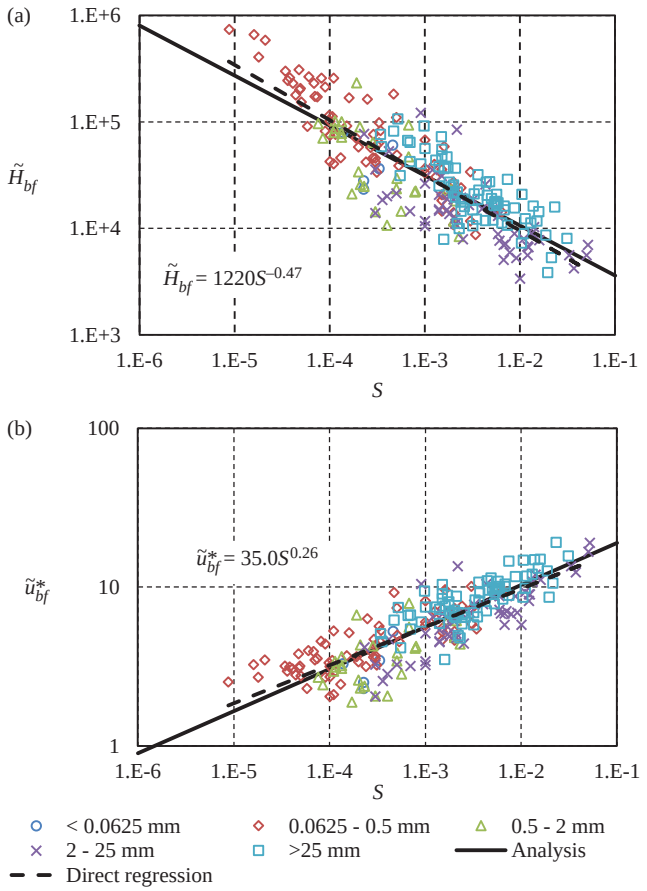

Figure 3 (a) Dimensionless bankfull depth $\tilde{H}_{bf} = H_{bf}g^{1/3}/(Rv)^{2/3}$ and (b) dimensionless bankfull shear velocity $u_{*bf} = u_{*bf}/(Rgv)^{1/3}$ versus bed slope. The dashed lines represent direct power-law fit of the data. The solid lines represent the relations described by Eq. (7a) and (7b), also displayed on the plots

be the result of spurious correlation. This, however, is not the case. Equation (7b) defines a relation between two independent dimensionless groupings, i.e. $H_{bf}g^{1/3}(Rv)^{2/3}$ and S. As shown in Fig. 3a, a direct regression of the data yields a relation that differs little from Eq. (7b). A regression line for dimensionless shear velocity is also shown in Fig. 3b; both regression lines are very close to Eq. (7a) and (7b), respectively.

Thus when bankfull shear velocity and bankfull depth are correlated against slope and grain size, they are (to first approximation) independent of grain size and dependent on the kinematic viscosity of water (in addition to slope). This conclusion would appear to contradict the results of a half-century of research on sediment transport dynamics and river morphology. Here we offer a hypotheses for the resolution of the conundrum of kinematic viscosity dependence. Our hypothesis is related to the existence of the floodplain itself. Bankfull depth is described by the sum of the thickness of the lower noncohesive layer in the floodplain (here characterized by D) and the upper thickness of finer material emplaced by floodplain deposition from wash load (Lauer and Parker 2008, Parker *et al.* 2011).

There is likely at least one "hidden" variable in the data of Fig. 2 which gives rise to the form of Eq. (5) for bankfull Shields number, and thus the dependency on viscosity, but lack of dependency on grain size in Eq. (7a) and (7b) for bankfull shear velocity and bankfull slope. The grain size D used in the analysis is a characteristic size of the bed material. There is a second, often much smaller size that characterizes the bank and floodplain material, here denoted as D_{bank}. This parameter also characterizes the size of the sediment suspended in the upper layer of the water column that spills onto, and emplaces the floodplain when the river goes overbank. As seen from Fig. 1, this size is likely to be less than 0.5 mm. It is thus in a grain size range where fall velocity is a strong function of Reynolds number. More specifically, dimensionless fall velocity $R_{f,bank} = v_{s,bank}/(RgD_{bank})$, where $v_{s,bank}$ is the fall velocity associated with a characteristic diameter of the size D_{bank}, is related to $D^*_{bank} = (Rg)^{1/3}D_{bank}/\nu^{2/3}$ through standard relations for fall velocity (e.g. Dietrich 1982). For example, Eq. (7a) can be rewritten as

$$\frac{u_{*bf}}{\sqrt{RgD_{bank}}} = 35.0\left(D^*_{bank}\right)^{-1/2} S^{0.26} \tag{9}$$

thus illustrating how viscosity can enter the problem across scales.

An independent data set on gravel-bed rivers is available to evaluate the hypothesis of viscosity dependence via fine-grained material from which the floodplain is constructed. The data set of Hey and Thorne (1986) includes 62 river reaches, divided into four classes, Vegetation Types I–IV in accordance to increasing bank height and floodplain vegetation density. In addition to the parameters specified above, that data also include bank material size D_{bank} for 58 of the reaches. Hey and Thorne (1986) indicate that higher vegetation density correlates with narrower and deeper reaches. It is a reasonable inference that narrower and deeper reaches have thicker floodplains characterized by the size D_{bank} rather than bed material size D.

We first demonstrate that the data of Hey and Thorne (1986) show the same pattern as the data used above. Figure 4a is a version of Fig. 2, but in which the new data set has been included. For each Vegetation Type the data are further partitioned between channels with bed material greater than 25 mm (D > 25 mm in Figs. 4 and 5) and channels with bed material finer than 25 mm (D < 25 mm in Figs. 4 and 5). The new data clearly follow the same trend as the previously used data, to which Eq. (5) provides a good fit. Figure 4b shows an expanded view of Fig. 4a in which only the new data are plotted. Figure 4b shows a tendency for $\tau^*_{bf}/S^{0.53}$ to increase with increasing vegetation density. This can be inferred to be associated with thicker floodplains emplaced by fine-grained material versus D^* for their data, along with Eq. (5). It is seen that the data generally follow Eq. (5), but also show a tendency related to floodplain thickness. That is, the value of $\tau^*_{bf}/S^{0.53}$ increases with increasing vegetation density.

Figures 5a and 5b are versions of Figs. 3a and 3b in which the new data have been added. Again, the data fit well within previous data, and Eq. (7a) and (7b) provides reasonable fits. Thus the new data tend to confirm the result that bankfull shear velocity

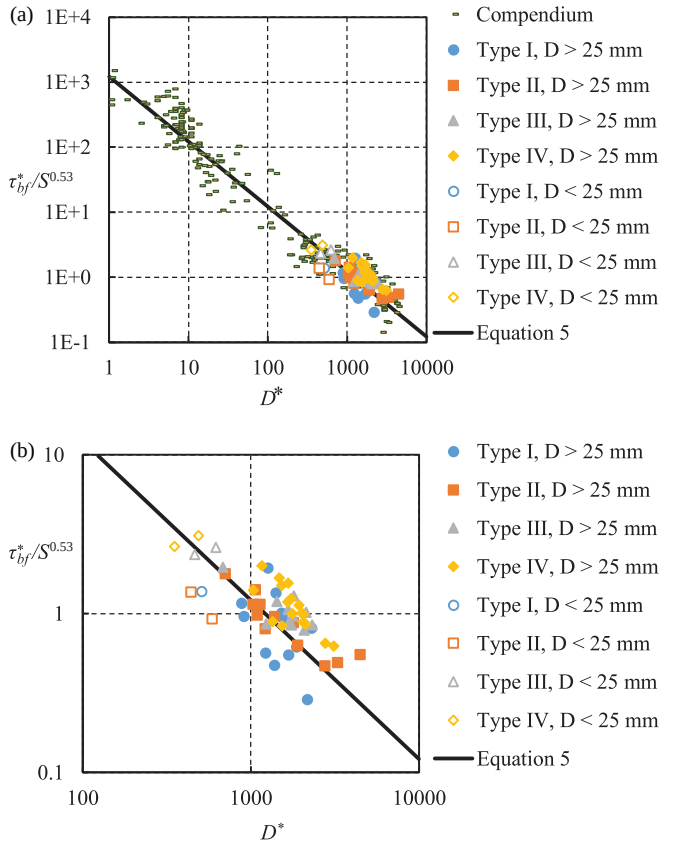

Figure 4 (a) Similarity collapse for $\tau^*_{bf}/S^{0.53}$ versus D^*, including the data set of Hey and Thorne (1986). Types I–IV represent the four classes of bank and floodplain vegetation density, with Type I having the lowest bank height and least floodplain vegetation density, and Type IV having the highest bank height and greatest floodplain vegetation density. The solid line represent Eq. (5) and (b) expanded view of Fig. 4a

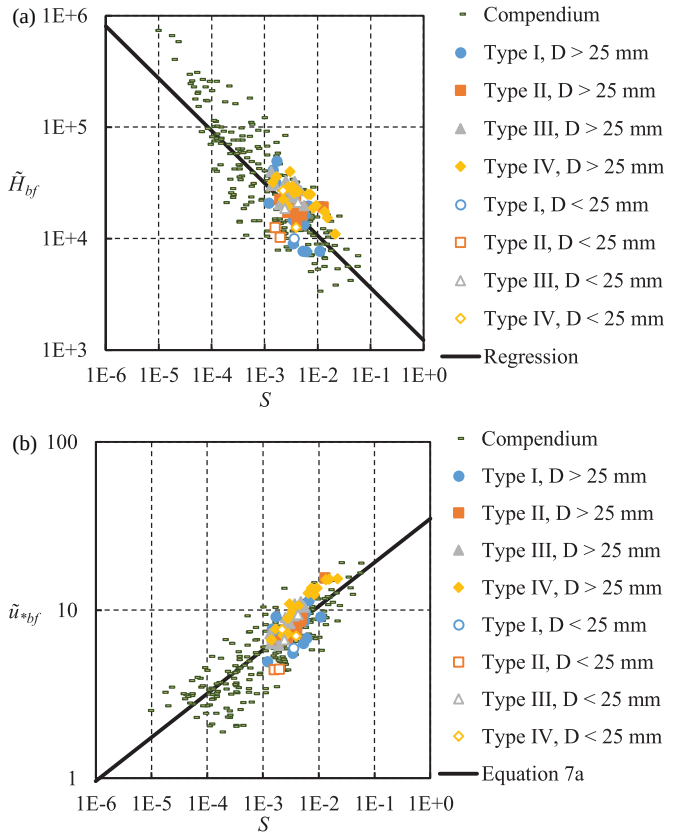

Figure 5 (a) Dimensionless bankfull depth $\tilde{H}_{bf} = H_{bf} g^{1/3}/(Rv)^{2/3}$, including the data set of Hey and Thorne (1986). Types I–IV represent the four classes of bank and floodplain vegetation density, with Type I having the lowest bank height and least floodplain vegetation density, and Type IV having the highest bank height and greatest floodplain vegetation density and (b) dimensionless bankfull shear velocity $\tilde{u}_{*bf} = u_{*bf}/(Rgv)^{1/3}$ versus bed slope, also including the data set of Hey and Thorne (1986). The solid lines represent the relations described by Eq. (7a) and (7b), also displayed on the plots

and bankfull depth are, to first order, dependent on viscosity but independent of bed material grain size.

Figure 6 shows a plot of dimensionless fall velocity $R_f = v_s/(RgD)^{1/2}$ versus $D^* = (Rg)^{1/3}D/v^{2/3}$, where here v_s is an arbitrary fall velocity and D is an arbitrary grain size. The curve shown therein is that of Dietrich (1982). Also shown on the plot are the values of $R_{f,bank}$ computed from the same relation, using the grain size D_{bank} from the 58 reaches of the Hey and Thorne (1986) for which D_{bank} is specified. It is important to keep in mind that Fig. 6 is not a comparison of measured versus predicted values. Instead, it shows that over the entire range of the data of Hey and Thorne (1986), the fall velocity of the bank/floodplain material can be expected to be strongly dependent on viscosity. It follows that bankfull Shields number and bankfull depth can be expected to include a viscosity dependence, as long as fine-grained material plays a substantial role in building the floodplain that confines the channel.

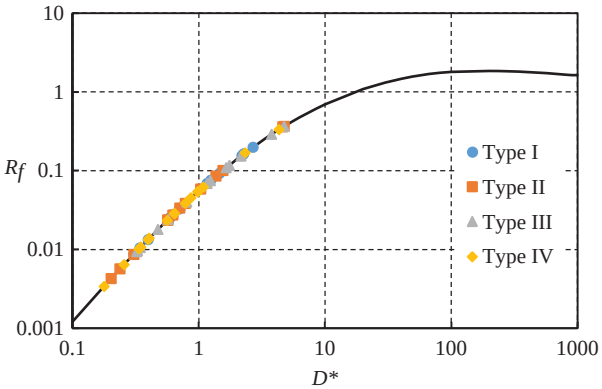

Figure 6 Dimensionless fall velocity $R_f = v_s/(RgD)^{1/2}$ versus dimensionless grain size $D^* = (Rg)^{1/3}D_k/v^{2/3}$, from the relation of Dietrich (1982). The points represent values of $R_{f,bank}$ computed from the same relation, using the bank/floodplain grain sizes D_{bank} from Hey and Thorne (1982)

4 General relations for bankfull characteristics

The characteristic grain size of the bed material D, however, does indeed enter the picture through predictive relations for H_{bf}, B_{bf}, and S as functions of Q_{bf} and Q_{tbf}. Such relations can be derived by augmenting Eq. (5) with (a) momentum balance

as approximated by Eq. (1); (b) the continuity relations

$$Q_{bf} = U_{bf} H_{bf} B_{bf} \tag{10a}$$

$$Q_{tbf} = q_{tbf} B_{bf} \tag{10b}$$

where U_{bf} is bankfull flow velocity and q_{tbf} is volume bed material transport rate per unit width at bankfull flow; (c) the definition of the dimensionless Chezy resistance coefficient Cz:

$$Cz = \frac{U_{bf}}{\sqrt{\tau_{bf}/\rho}} = \frac{U_{bf}}{u_{*bf}} \tag{11}$$

(d) a specification of Cz; and e) a predictor for q_{tbf}.

The calculations can be performed for any pair of relations for Cz and q_{tbf}. An example generic relation for q_{tbf} is

$$q_{tbf} = \sqrt{RgD} D \alpha_t \left[\varphi_s \tau^*_{bf} - \tau^*_c\right]^{n_t} \tag{12}$$

where α_t, φ_s, n_t are arbitrary coefficients and exponent of the sediment transport relation (Parker 2004). Equations (1), (2) and (10)–(12) can be reduced to produce the three relations for bankfull characteristics,

$$B_{bf} = \frac{1}{\alpha_t \left(\varphi_s \tau^*_{bf} - \tau^*_c\right)^{n_t} \sqrt{RgD} D} Q_{tbf} \tag{13}$$

$$H_{bf} = \frac{D \alpha_t \left(\varphi_s \tau^*_{bf} - \tau^*_c\right)^{n_t}}{\sqrt{\tau^*_{bf}} Cz} \frac{Q_{bf}}{Q_{tbf}} \tag{14}$$

$$S = \frac{\left(R\tau^*_{bf}\right)^{3/2} Cz}{\alpha_t \left(\varphi_s \tau^*_{bf} - \tau^*_c\right)^{n_t} \sqrt{R}} \frac{Q_{tbf}}{Q_{bf}} \tag{15}$$

Equations (13)–(15) cannot be solved explicitly in terms of simple power laws when τ^*_c is not equal to zero, because τ^*_{bf} is a function of S as specified by Eq. (5). In this case, an iterative technique may be useful to obtain a solution. The above relations are general, and apply for any specification for τ^*_{bf} and Cz. The constant Shields formulation is recovered by setting τ^*_{bf} and Cz to prescribed constants.

5 Relations for bankfull characteristics for sand-bed streams

In the case of sand-bed streams, the Engelund–Hansen total bed material load relation (Engelund and Hansen 1967),

$$q_{tbf} = \alpha_{EH} Cz^2 \sqrt{RgD} D \left(\tau^*_{bf}\right)^{5/2} \tag{16a}$$

$$\alpha_{EH} = 0.05 \tag{16b}$$

is used because it is accurate for sand transport (Brownlie 1981) and allows solution in closed form in terms of simple power laws that clearly elucidate the results.

The resistance coefficient Cz is often specified with a set value of Manning's n, but this is not reliable for, e.g. rivers dominated by bedform resistance (Ferguson 2010). The subset of the data used here corresponding to grain sizes between 0.0625 and 2 mm is thus used to find an empirical relation between Cz at bankfull flow and bed slope S. Figure 7 shows Cz versus S for the entire data set, as well as the regression relation

$$Cz = \alpha_R S^{-n_R} \tag{17}$$

where $\alpha_R = 2.53$ and $n_R = 0.19$, determined for the indicated subset. The data show substantial scatter, which is to be expected in light of, e.g. varying bedform regimes, bar configuration and channel sinuosity. Equation (17), however, captures the overall trend for Cz to decline with increasing S.

Equation (17) is an empirical relation that was first proposed in Chapter 3 of Parker (2004). As noted above, it is likely superior to a formulation using Manning's n, which needs to be guessed or determined from site-specific data for most rivers (Ferguson 2010).

Substituting Eqs. (5), (16a), (16b) and (17) into Eqs. (13)–(15), the following relations for bankfull characteristics of sand-bed streams with characteristic bed size ranging from very fine to medium sand result:

$$\frac{B_{bf}}{D} = \frac{(D^*)^{2.5}}{\alpha_{EH}\sqrt{R}\alpha_R^2 \beta^{2.5} \left[RD^*/\alpha_{EH}\alpha_R\beta\right]^{(2.5m-2n_R)/(1+m-n_R)}} \times \left(\frac{Q_{tbf}}{Q_{bf}}\right)^{-(2.5m-2n_R)/(1+m-n_R)} \frac{Q_{tbf}}{\sqrt{gD}D^2} \tag{18}$$

$$\frac{H_{bf}}{D} = \frac{\alpha_{EH}\alpha_R\beta^2}{(D^*)^2} \left[\frac{RD^*}{\alpha_{EH}\alpha_R\beta}\right]^{(2m-n_R)/(1+m-n_R)} \times \left(\frac{Q_{tbf}}{Q_{bf}}\right)^{(2m-n_R)/(1+m-n_R)} \frac{Q_{bf}}{Q_{tbf}} \tag{19}$$

$$S = \left[\frac{RD^*}{\alpha_{EH}\alpha_R\beta}\right]^{1/(1+m-n_R)} \left(\frac{Q_{tbf}}{Q_{bf}}\right)^{1/(1+m-n_R)} \tag{20}$$

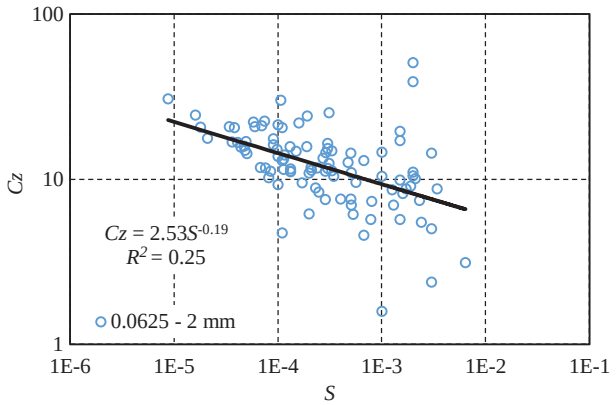

Figure 7 Plot of dimensionless Chezy resistance coefficient Cz at bankfull flow versus slope S. Data are shown for only two grain size ranges of Figs. 1 and 2, covering $D - 0.0625$ mm to 2 mm., i.e. very fine to medium sand. The regression relation shown in the figure, i.e. Eq. (17), was obtained only using data for $D - 0.0625$ mm to 2 mm

In light of Fig. 2, these relations have a much stronger empirical basis than corresponding relations presented elsewhere based on constant bankfull Shields number and Chezy resistance coefficient (Parker *et al.* 1998a, 2008, Parker 2004). The above relations have been used in a model of co-evolving river width and sinuosity in meandering rivers (Eke 2013), and can be used as the basis for improved morphodynamic models of channel-floodplain or channel-delta co-evolution (Kim *et al.* 2009).

6 Comparison of bankfull characteristics relations for sand-bed streams: from constant Shields number versus the proposed formulation

In the case of constant τ^*_{bf} and Cz, Equations (13)–(15) can be used to express the exponent dependency of H_{bf}, B_{bf}, and S on Q_{bf}, Q_{tbf}, and D:

$$B_{bf} \sim Q_{bf}^{0} Q_{tbf}^{1} D^{-1.5} \tag{21a}$$

$$H_{bf} \sim Q_{bf}^{1} Q_{tbf}^{-1} D^{1} \tag{21b}$$

$$S \sim Q_{bf}^{-1} Q_{tbf}^{1} D^{0} \tag{21c}$$

Similarly, exponents in Eqs. (18)–(20) for the proposed formulation, with $m = 0.53$ and $n_R = 0.19$, as determined for Eqs. (5) and (17), are, respectively:

$$B_{bf} \sim Q_{bf}^{0.71} Q_{tbf}^{0.29} D^{0.29} \tag{22a}$$

$$H_{bf} \sim Q_{bf}^{0.35} Q_{tbf}^{-0.35} D^{-0.35} \tag{22b}$$

$$S \sim Q_{bf}^{-0.75} Q_{tbf}^{0.75} D^{0.75} \tag{22c}$$

The resulting equations with: constant bankfull Shields number, i.e. Eq. (21a)–(21c), and the proposed relations, i.e. Eq. (22a)–(22c) gives fundamentally different predictions for B_{bf}, H_{bf}, and S.

In the proposed formulation, (a) bankfull width increases with increasing flood discharge, sand supply and sand size (with the respective exponents 0.71. 0.29 and 0.29); (b) bankfull depth increases with increasing flood discharge, and decreasing sand supply and sand size (with the respective exponents 0.35, −0.35 and −0.35); and (c) slope increases with decreasing flood discharge, and increasing sand supply and sand size (with respective exponents −0.75, 0.75 and 0.75).

It is useful to recall that the correlation of bankfull Shields number with slope and grain size specified by Eq. (5) dictates that bankfull shear velocity and bankfull depth are independent of grain size (Eqs. 7 and 8). Equation (22a)–(22c), however, indicates that when slope, bankfull width and bankfull depth are expressed as functions of the three parameters bankfull discharge, sediment transport rate at bankfull discharge and grain size, all the relations show a dependence on grain size. This is because grain size enters the formulation via Eq. (5) for bankfull Shields number and Eq. (16) for bed material transport rate, in both cases as the inverse of grain size.

The constant bankfull Shields formulation of Eq. (21a) suggests that B_{bf} is independent of Q_{bf} (with an exponent of 0) and strongly decreases with an increase in the median grain size diameter (with an exponent of −1); this is quite divergent from our proposed Eq. (22a) which shows strongest dependence on flood discharge (exponent of 0.71). In addition, the dependency H_{bf} on Q_{bf} and Q_{tbf} on H_{bf} with our proposed Eq. (22b) is such that the magnitude of the exponents are reduced by a factor of nearly three as compared to Eq. (21b) for constant Shields number. The dependence of S on Q_{bf} and Q_{tbf} in our proposed relation (22c) is similar to the constant Shields number Eq. (21c), but the magnitude of the exponents are muted. Our proposed Eq. (22c) shows a strong dependence of S on grain size (exponent of 0.75) whereas the constant Shields number Eq. (21c) is independent of grain size.

7 Application to morphodynamic modeling: case of the Fly-Strickland River system, Papua New Guinea

The proposed relations for bankfull characteristics (i.e. Eqs. 18–20) can be used to model morphologic changes of a self-formed channel and adjacent floodplain. In order to do this, it must be assumed that the change of a self-formed channel is slow enough that floodplain morphology can keep up with it, so that the channel neither avulses during aggradation or strongly incises during degradation.

Our relations for τ^*_{bf} and Cz, i.e. Eqs. (5) and (17), represent regression of data with the scatter shown in Figs. 2 and 7. Thus in any application to a specific river, it is appropriate to normalize Eqs. (5) and (17) relative to a known reference slope S_R, at which τ^*_{bf} takes the known reference value τ^*_R and Cz takes the known reference value Cz_R. With this in mind, Eqs. (5) and (17) are normalized to the respective forms

$$\tau^*_{bf} = \tau^*_R \left(\frac{S}{S_R}\right)^{m} \tag{23}$$

$$Cz = Cz_R \left(\frac{S}{S_R}\right)^{-n_R} \tag{24}$$

where the exponents m and n_R are those of Eqs. (5) and (17), respectively. These exponents maintain the trends captured in empirical relations, but emanate from a single data point rather than regressed average of all data points. We re-evaluate Eqs. (18)–(20) with Eqs. (23) and (24) to the forms

$$\frac{B_{bf}}{D} = \frac{1}{\alpha_{EH}\sqrt{R}Cz_R^2\tau_R^{*2.5}\left[R/\alpha_{EH}S_R Cz_R \tau_R^*\right]^{(2.5m-2n_R)/(1+m-n_R)}} \times \left(\frac{Q_{tbf}}{Q_{bf}}\right)^{-(2.5m-2n_R)/(1+m-n_R)} \frac{Q_{tbf}}{\sqrt{gD}D^2} \tag{25}$$

$$\frac{H_{bf}}{D} = \alpha_{EH} Cz_R \tau_R^{*2} \left[\frac{R}{\alpha_{EH} S_R Cz_R \tau_R^*}\right]^{(2m-n_R)/(1+m-n_R)} \times \left(\frac{Q_{tbf}}{Q_{bf}}\right)^{(2m-n_R)/(1+m-n_R)} \frac{Q_{bf}}{Q_{tbf}} \quad (26)$$

$$S = \left[\frac{RS_R^{m-n_R}}{\alpha_{EH} Cz_R \tau_R^*}\right]^{1/(1+m-n_R)} \left(\frac{Q_{tbf}}{Q_{bf}}\right)^{1/(1+m-n_R)} \quad (27)$$

Parker *et al.* (2008b) and Lauer *et al.* (2008) have studied the response of the Fly-Strickland River system to Holocene sea level rise due to deglaciation of 10 mm/year for 12,000 years. Large, low-slope rivers worldwide show the imprint of this rise. Parker *et al*. (2008b) analysed the problem in the context of the constant Shields number model for hydraulic geometry. Here we show the differences in the results that arise when we instead apply our proposed model.

The Fly-Strickland River system in Papua New Guinea drains an area of approximately 75,000 km^2 and consists of the Strickland River, Fly River and tributaries such as the Ok Tedi (Fig. 8). The Fly River is segmented into the Upper Fly, Middle Fly, and Lower Fly, bounded by junctions with the Ok Tedi and Strickland Rivers, respectively. The confluence of the Fly and the Strickland rivers is called Everill Junction (Parker *et al.* 2008).

The Fly-Strickland River system begins in the highlands, where the streams are dominated by bedrock and gravel-bed morphologies. Farther downstream, as the slope gradient decreases, both the Fly and Strickland rivers transition into fully alluvial gravel bed-streams (Parker *et al.* 2008). Even farther downstream, the two rivers transition into low-gradient sand-bed streams about 240 km upstream of Everill Junction (Parker *et al.* 2008) and approximately 600 km upstream of the modern delta (Lauer *et al.* 2008). Here, we consider only the sand-bed portion, downstream from the gravel-sand transition but upstream of the tidally influenced delta. The Fly-Strickland River is selected for this study because of its relatively homogeneous climatic and sea level forcing (Lauer *et al.* 2008) and the availability of data.

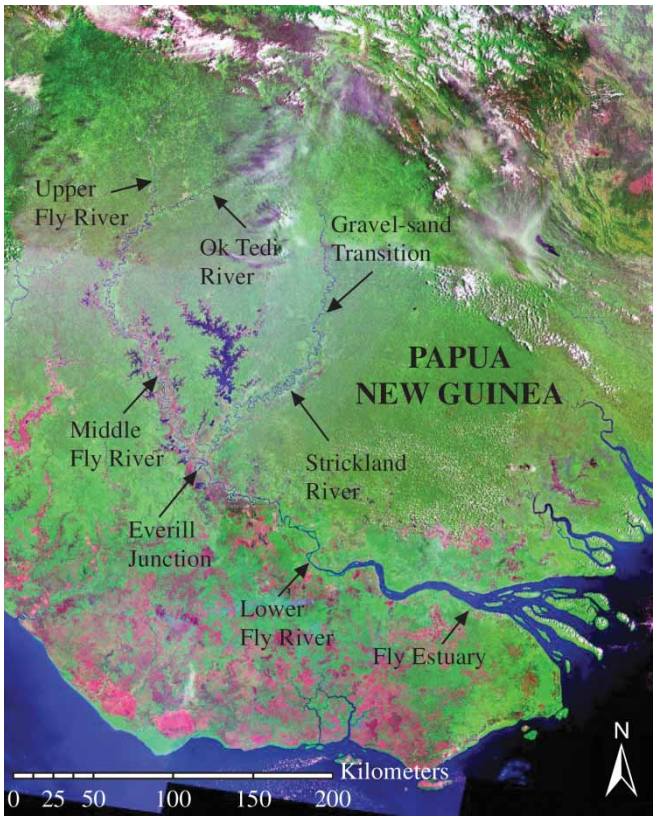

Figure 8 Aerial view of the Fly-Strickland River system, from 1987–1994 NASA/USGS Landsat TM data. The study reach extends from the gravel-bed transition to 200 km downstream

Parker *et al.* (2008) present a model for self-formed rivers using bankfull characteristics of the Fly-Strickland River system and a constant bankfull Shields number $\tau_{bf}^* = 1.82$. In their model, the portions of the Middle Fly and Strickland rivers between the gravel-sand transition and the Everill Junction are combined into a single reach for simplicity. We use this assumption and identical parameters, but also include reference values selected from Parker *et al.* (2008) at the most upstream point of the modelled reach, i.e. just downstream of the sand-gravel transition of the Strickland River. These parameters, some of which are defined below, are specified in Table 1.

Our analysis differs from that of Parker *et al.* (2008) in regard to the downstream of the reach. In Parker *et al.* (2008), the reach ends in a delta, which may advance or retreat depending on sediment supply and the rate and duration of sea level change. In the work presented here, the location of the downstream end is held constant for simplicity, but the bed elevation there is allowed to vary in accordance with the sea level change (Parker 2004). We apply this constraint to both the case of constant

Table 1 Fly-Strickland River system model parameters, from Parker *et al.* (2008)

Parameter	Value	Units	Descriptions
Q_{bf}	5700	m^{3}s^{-1}	Bankfull water discharge
I_f	0.175	–	Flood intermittency
Q_{tbff}	0.80	m^{3}s^{-1}	Sand feed rate during floods
Λ	1.0	–	Mud/sand deposition ratio
Ω	2.0	–	Channel sinuosity
D	0.25	mm	Characteristic sand grain size
B_f	12,000	m	Floodplain width
λ_p	0.35	–	Porosity of channel/floodplain complex
R	1.65	–	Submerged specific gravity of sediment
ξ_d	10	mm/year	Rate of sea level rise
S_R	0.0001	–	Reference slope at sand-gravel transition
τ_R^*	1.82	–	Reference bankfull Shields number
Cz_R	25	–	Reference Chezy friction factor

bankfull Shields number and our proposed formulation with variable bankfull Shields number.

Parker (2004) outlines the steady-state analytical (closed-form) solution for the river profile under a constant rate of sea level rise. It is this steady-state analytical (closed-form) solution that we seek here. As opposed to the backwater formulation of Parker *et al.* (2008), we use the normal flow formulation of Parker (2004) for simplicity. The Exner equation is used for sediment conservation, accounting for channel sinuosity, flood intermittency, floodplain width, and mud deposition. It is assumed that morphodynamically significant sediment transport takes place only during floods (Nittrouer *et al.* 2011). The model assumes that sediment is transported within the channel, but is deposited evenly across the channel-floodplain complex as the channel reworks the floodplain by migration (Lauer and Parker 2008). The resulting form for the Exner equation is

$$\frac{\partial \eta}{\partial t} = -\frac{I_f \Omega (1+\Lambda)}{(1-\lambda_p) B_f} \frac{\partial Q_{tbf}}{\partial x} \tag{28}$$

where η is bed elevation, t is time, I_f is the flood intermittency (the fraction of time that the river is in flood), Ω is channel sinuosity, Λ is a ratio defined as the fraction of mud deposited in the channel-floodplain complex per unit sand deposited, λ_p is porosity of channel/floodplain sediment deposit, B_f is floodplain width, and x is the downstream coordinate (Parker *et al.* 2008).

Downstream bed elevation is set to sea level, that is,

$$\eta(L,t) = \xi_{do} + \dot{\xi}_d t \tag{29}$$

where L is the reach length, ξ_{do} is the initial sea level elevation, and ξ_d is an assumed constant rate of sea level rise. Furthermore, bed elevation $\eta(x,t)$ is represented in terms of downstream bed elevation and the deviation $\eta_{dev}(x,t) = \eta - \eta(L,t)$, such that

$$\eta = \xi_{do} + \dot{\xi}_d t + \eta_{dev}\,(x,t) \tag{30}$$

Under steady-state condition relative to the sea level, $\partial \eta_{dev}/\partial t = 0$, thus Eqs. (28) and (30) reduce to

$$\dot{\xi}_d = -\frac{I_f \Omega (1+\Lambda)}{(1-\lambda_p) B_f} \frac{\partial Q_{tbf}}{\partial x} \tag{31}$$

Here we calculate the bed material load Q_{tbf} with Eq. (31), and then B_{bf}, H_{bf} and S are calculated by Eqs. (25)–(27) for our proposed model with varying bankfull Shields number, and by Eqs. (18)–(20) with τ^*_{bf} and Cz held constant to the reference values of Table 1, and $\varphi_s = 1$, $\tau^*_c = 0$, $n_t = 2.5$ and $\alpha_t = \alpha_{EH}$ (Engelund–Hansen relation).

Modeling results for steady-state bankfull width, bankfull depth, bed slope, and deviatoric bed elevation are shown in Figs. 9–12. In the case of constant bankfull Shields number, the bankfull depth increased from 7.38 to 62.9 m over 200 km of channel, equivalent to an unrealistic 850% increase (Fig. 10);

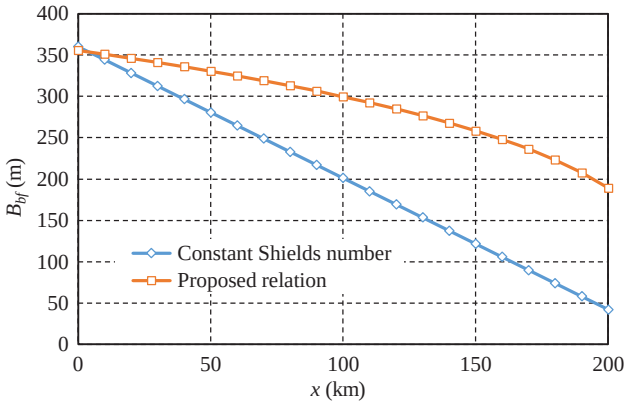

Figure 9 Model predictions for the downstream variation of bankfull width for the Fly-Strickland River system under conditions of steady-state response to constant sea level rise. Results are shown for both the constant bankfull Shields number model and our proposed variable bankfull Shields number model

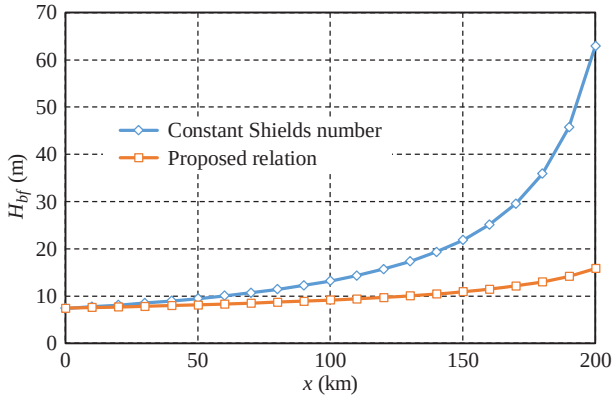

Figure 10 Model predictions for the downstream variation of bankfull depth for the Fly-Strickland River system under conditions of steady-state response to constant sea level rise. Results are shown for both the constant bankfull Shields number model and our proposed variable bankfull Shields number model

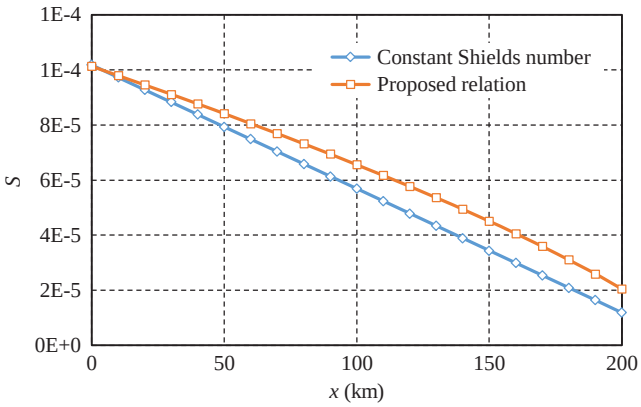

Figure 11 Model predictions for the downstream variation of bed slope for the Fly-Strickland River system under conditions of steady-state response to constant sea level rise. Results are shown for both the constant bankfull Shields number model and our proposed variable bankfull Shields number model

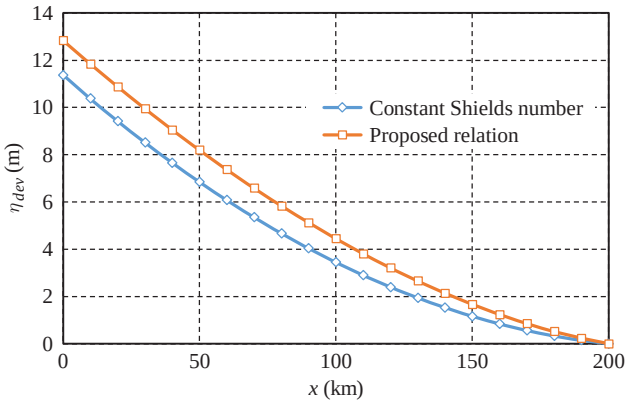

Figure 12 Model predictions for the downstream variation of deviatoric bed elevation for the Fly-Strickland River system under conditions of steady-state response to constant sea level rise. Results are shown for both the constant bankfull Shields number model and our proposed variable bankfull Shields number model

the majority of this change occurs over the last quarter length of the channel as depth increases. Our proposed formulation with variable bankfull Shields number shows a more muted increase in bankfull depth, from 7.46 m at the upstream end to 15.8 m at the outlet. Both cases are shown in Fig. 10.

Bankfull width linearly decreases by 88% (360.2–42.2 m) in the constant bankfull Shields number formulation, but non-linearly decreases only by 53% (355.7–189.1 m) with the proposed variable Shields number formulation (Fig. 9). Corresponding widths extracted from the most recent Google Earth image are 420 and 300 m, corresponding to a 29% decrease (Table 2). Both cases are shown in Fig. 9. The variable Shields number formulation is clearly more in accord with the data. A major part of the discrepancy between the observed percentage width decrease and that predicted by our proposed model is likely due to the fact that the model results assume constant sea level rise of 10 mm/year, whereas in reality the rate of sea level rise had changed in time.

The differences in slope and bed elevation profile predicted by the two models are relatively weak, but still evident (Figs. 11 and 12). The proposed relation results show a metre or more difference in bed elevation between the two models over the first 100 km of studied reach. Previous results using the constant bankfull Shields number model paired with Exner equation gave adequate values for bed elevation (Parker *et al.* 2008), but unrealistically strong downstream variation in width and depth.

Figures 13 and 14 plot the results for both models over observed data of Figs. 2 and 7, respectively. Figure 13 shows the upstream (reference) and downstream values of $\tau^*_{bf}/S^{0.53}$ versus dimensionless grain size D^*, and Fig. 14 shows the upstream (reference) and downstream values of Cz against the corresponding values for bed slope S. In the case of constant bankfull Shields number τ^*_{bf} remains constant. In the case of our proposed variable bankfull Shields number model, τ^*_{bf} increases downstream, the upstream value is at the middle of the scatter of the data, and the downstream value is only slightly outside of it. In the case of Cz, the results of our model follow the trend of the data, whereas the constant Shield stress model does not. In both figures, however, the values for both models fit within the scatter of the data.

Table 2 Measurements of bankfull channel widths (in kilometres) of the Fly-Strickland River system, at the gravel-bed transition and just upstream of Everill Junction, from 4 September 2013 Google Earth Landsat image

Measurement	Gravel-sand transition (km)	Just upstream of Everill Junction (km)
1	0.48	0.32
2	0.41	0.33
3	0.38	0.28
4	0.42	0.28
5		0.3
Average	0.4225	0.302

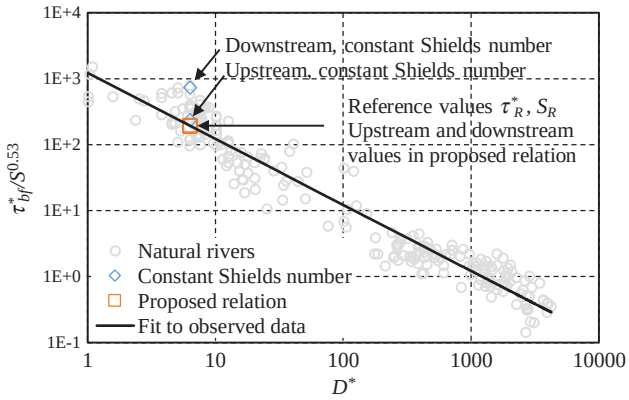

Figure 13 Results of the steady-state model for Shields number subject to constant sea level rise, plotted with the data and regression line of Fig. 2. The arrows show the reference values of τ^*_{bf} at the upstream end of the reach, and the upstream and downstream values of τ^*_{bf} in the constant and our proposed variable bankfull Shields number models. The downstream value for τ^*_{bf} for the proposed bankfull Shields stress model is the same as the upstream value

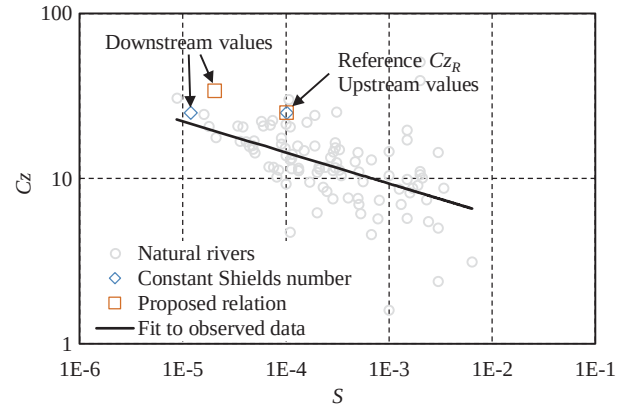

Figure 14 Results of the steady-state model for Chezy friction coefficient Cz subject to constant sea level rise, plotted with the data and regression line of Fig. 7. The arrows show the reference values of Cz at the upstream end of the reach, and the downstream values predicted by both the constant and variable bankfull Shields number models

8 Discussion: application to modern sea level rise driven by climate change

The model presented here has direct application to modern sea level rise associated with climate change. Figure 15 shows the range of predictions for sea level rise over the century from 2000 to 2100, as specified in the UN Intergovernmental Panel on Climate Change (IPCC 2013). The indicated values correspond to average rates of sea level rise ranging from 2.8 to 9.8 mm/year. Our proposed variable Shields number model, applied in the context of Parker *et al.* (2008) for which a river ends in a delta, is directly applicable to the prediction of the response of river profiles to modern sea level rise. Indeed, the high end of sea level rise nearly equals to rate 10 mm/year used herein for the case of the Fly-Strickland River system.

Certain of the results obtained in Section 6 deserve emphasis. In the constant Shields number formulation, slope is independent of grain size, whereas in our proposed formulation slope strongly increases with grain size. We speculate that the latter result is more reasonable. In the constant Shields number formulation, bankfull width is independent of bankfull discharge, whereas in our proposed formulation bankfull width increases strongly with bankfull discharge. Again, we speculate that the latter result is more reasonable.

In the present application of the model, grain size D is held constant at 0.25 mm. In reality, however, large sand-bed rivers typically show a tendency for downstream fining of grain size, which may result in a somewhat stronger increase of the bankfull Shields number and in a better prediction of the streamwise changes in bankfull channel geometry. In order to account for this effect, it is necessary to consider a grain size mixture and allow for selective deposition. The methodology for this is specified in Wright and Parker (2005a, 2005b).

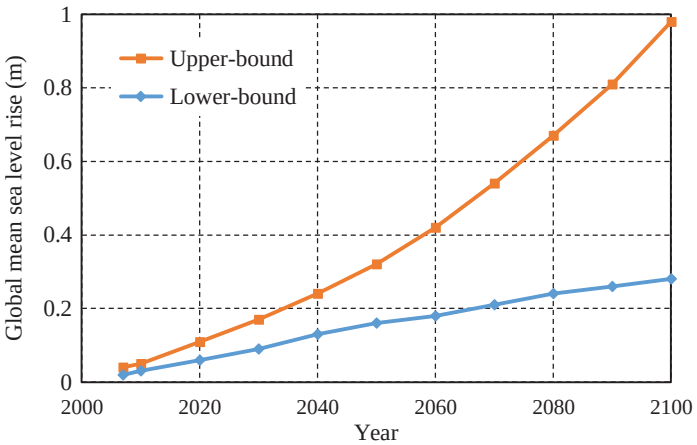

Figure 15 Range of predictions for sea level rise over the century spanning 2000 and 2100, as indicated in the most recent report of the UN Intergovernmental Panel on Climate Change (IPCC 2013). The predictions correspond to average rates of sea level rise ranging from 2.8 to 9.8 mm/year

9 Conclusions

Previous relations for the dependency of bankfull width, bankfull depth and bed slope have been based on the assumption of constant formative bankfull Shields number. Here we show that this assumption does not adequately represent the data. We propose a new relation for which bankfull formative Shields number is a variable. The implications of our proposed relation are as follows.

- Empirical analysis of measured data from natural rivers show that the bankfull, or formative Shields number can be accurately described as a universal function of slope and grain size than by a constant value. This function was determined from a data base including 230 river reaches, with bankfull discharge varying from 0.34 to 216,340 m^3s^{-1}, bankfull width varying from 2.3 to 3400 m, bankfull depth varying from 0.22 to 48.1 m, bed slope varying from 8.8×10^{-6} to 5.2×10^{-2}, and characteristic bed grain size varying from 0.04 to 168 mm.
- This relation gives the unexpected result that when bankfull shear velocity and bankfull depth are computed from the relation for bankfull Shields number, they are dependent on kinematic viscosity of water but independent of bed material grain size.
- The dependence of bankfull shear velocity on viscosity may be due to the presence of fine-grained suspended sediment load in the system, the characteristic grain size of which is not represented by the characteristic grain size of the bed material. The fall velocity of fine sand and silt is strongly dependent on viscosity, and it is from this material that much of the floodplain is constructed.
- Bed material grain size, does, however, enter in the predictive relations for bankfull depth, bankfull width and bed slope as functions of bankfull discharge and bankfull total bed material load.
- The proposed relation for bankfull Shields number can be implemented into a model for the long profiles of bankfull width, bankfull depth, bed slope and bed elevation self-formed channels using, relations derived from: (a) our proposed empirical relation for bankfull Shields number, which varies with slope and grain size, (b) momentum balance, (c) continuity, (d) a relation for resistance coefficient, and (e) a bed material load transport relation.
- Models using the constant bankfull Shields number formulation, applied to the case constant sea level rise at a rate of 10 mm/year associated with Holocene deglaciation, predict long profiles for which bankfull depth and width increase unrealistically in the downstream direction. A more reasonable pattern is predicted from our proposed variable bankfull Shields number formulation.
- Our new model is directly applicable to the prediction of river response to modern sea level rise associated with climate change. Predicted rates of sea level rise range from 2.8

to 9.8 mm/year, the upper bound corresponding to the case modelled here.

Acknowledgements

Input from Brandon McElroy is very much appreciated.

Funding

This research was supported by the United States National Science Foundation, through Award Numbers 1209427 (WSC-Category 2) 1135427 (FESD Type I) and DGE 11-44245 (Graduate Research Fellowship Program).

Notation

B_{bf} = bankfull width (m)
B_f = floodplain width (km)
Cz = dimensionless Chezy coefficient (−)
Cz_R = reference dimensionless Chezy coefficient (−)
D = bed material grain size (mm)
D_{bank} = characteristic size of fine-grained sediment in the banks and floodplain (mm)
D^* = $(Rg)^{1/3}D/\nu^{2/3}$ = dimensionless grain size of bed material (−)
D^*_{bank} = $(Rg)^{1/3}D_{bank}/\nu^{2/3}$ = dimensionless grain size of bank/floodplain material (−)
g = acceleration of gravity (ms^{-2})
H_{bf} = bankfull depth (m)
$\tilde{H}_{bf}$ = dimensionless depth (−)
I_f = flood intermittency (−)
L = reach length (km)
m = exponent in the proposed bankfull Shields relation (−)
n_t = exponent of an example sediment transport relation (−)
n_R = exponent of the relation for dimensionless Chezy coefficient (−)
Q_{bf} = bankfull discharge (m^3s^{-1})
Q_{tbf} = total volume bed material load at bankfull flow (m^3s^{-1})
q_{tbf} = volume bed material transport rate per unit width at bankfull flow (m^2s^{-1})
R = submerged specific gravity of sediment (−)
$R_{f,bank}$ = $v_{s,bank}/(RgD_{bank})^{1/2}$, dimensionless fall velocity of bank/floodplain material (−)
S = bed slope (−)
S_R = reference slope (−)
t = time (s)
U_{bf} = bankfull flow velocity (ms^{-1})
u_{*bf} = bankfull shear velocity (ms^{-1})
$\tilde{u}_{*bf}$ = dimensionless shear velocity (−)
v_s = sediment fall velocity
$v_{s,bank}$ = fall velocity of fine-grained bank/floodplain material (ms^{-1})
x = downstream coordinate (km)
α_{EH} = coefficient of the Engelund–Hansen load relation (−)
α_R = coefficient of the relation for dimensionless Chezy coefficient (−)
α_t = coefficient of an example sediment transport relation (−)
β = coefficient in the proposed bankfull Shields relation (−)
η = bed elevation (m)
η_{dev} = deviatoric bed elevation (m)
Λ = mud/sand deposition ratio (−)
λ_p = porosity of the channel/floodplain bed sediments (−)
ν = kinematic viscosity of water (ms^{-2})
ξ_{do} = initial sea level elevation (m)
ξ_d = assumed rate of sea level rise (mm/year)
ρ = water density (kgm^{-3})
τ^*_{bf} = formative (bankfull) channel Shields number (−)
τ^*_c = critical Shields number (−)
τ^*_R = reference formative (bankfull) channel Shields number (−)
φ_t = coefficient of an example sediment transport relation (−)
Ω = channel sinuosity (−)

The supplemental data for this article can be accessed at http://hydrolab.illinois.edu/people/parkerg//VariableShieldsModelBasicData.htm.

References

Brownlie, W.R. (1981). Prediction of flow depth and sediment discharge in open channels. *Report No. KH-R-43A*, W.M. Keck Laboratory of Hydraulics and Water Resources, California Institute of Technology, Pasadena, CA, http://caltechkhr.library.caltech.edu/7/01/KH-R-43A.pdf.

Dade, W.B., Friend, P.F. (1998). Grain-size, sediment-transport regime, and channel slope in alluvial rivers. *J. Geology* 106, 661–675.

Dietrich, W.E. (1982). Settling velocity of natural particles. *Water Resour. Res.* 18(6), 1615–1626.

Eke, E.C. (2013). Numerical modeling of river migration incorporating erosional and depositional bank processes. *PhD Thesis*. Department of Civil and Environmental Engineering, University of Illinois Urbana-Champaign, IL.

Engelund, F., Hansen, E. (1967). *A monograph on sediment transport in alluvial streams*. Technisk Vorlag, Copenhagen.

Ferguson R. (2010). Time to abandon the manning equation? *Earth Surf. Proc. Land* 35, 1873–1876.

Hey, R.D., Thorne, C.R. (1986). Stable channels with mobile gravel beds. *J. Hydraulic Eng.* 112(6), 671–689.

IPCC. (2013). Climate change 2013: The physical science basis. *Report*, U.N. Intergovernmental Panel on Climate Change, http://www.climatechange2013.org/

Kim, W., Mohrig, D., Twilley, R., Paola, C., Parker, G. (2009). Is it feasible to build new land in the Mississippi River delta? *EOS* 90(42), 373–374.

Lamb, M.P., Dietrich, W.E., Venditti, J.G. (2008). Is the critical Shields stress for incipient sediment motion dependent on channel-bed slope? *J. Geophys. Res.* 113(F02008).

Latrubesse, E.M. (personal communication). Data base for large tropical rivers. latrubesse@austin.utexas.edu

Lauer, J.W., Parker, G. (2008). Net local removal of floodplain sediment by river meander migration. *Geomorphology* 96(1–2), 123–149.

Lauer, J.W., Parker, G., Dietrich, W.E. (2008). Response of the Strickland and Fly River confluence to postglacial sea level rise. *J. Geophys. Res.* 113(F01S06).

Leopold, L.B., Maddock, Jr., T. (1953). The hydraulic geometry of stream channels and some physiographic implications. In *Professional paper 252*. U.S. Geological Survey, Washington, DC.

Mueller, E.R., Pitlick, J. (2005). Morphologically based model of bed load transport capacity in a headwater stream. *J. Geophys. Res.* 110, 14, doi:10.1029/2003JF000117

Nittrouer, J.A., Mohrig, D., Allison M.A. (2011). Punctuated sand transport in the lowermost Mississippi River. *J. Geophys. Res.* 116, 1914–1934, doi:10.1029/2011JF002026

Paola, C., Heller, P.L., Angevine, C.L. (1992). The large-scale dynamics of grain-size variation in alluvial basins, 1: Theory. *Basin Res.* 4, 73–90.

Parker, G. (1978). Self-formed straight rivers with equilibrium banks and mobile bed. Park 2. The gravel river. *J. Fluid Mech.* 89, 127–146.

Parker, G. (2004). *1D sediment transport morphodynamics with applications to rivers and turbidity currents* (E-book; http://vtchl.uiuc.edu/people/parkerg/).

Parker, G. (2008). Transport of gravel and sediment mixtures. In *Sedimentation engineering. Processes, measurements, modeling and practice.* M.H. Garcia, ed. ASCE, Reston, VA, chap. 3, 165–251.

Parker, G., Paola, C., Whipple, K.X., Mohrig, D. (1998a). Alluvial fans formed by channelized fluvial and sheet flow. I: Theory. *J. Hydraulic Eng.* 124(10), 985–995.

Parker, G., Paola, C., Whipple, K.X., Mohrig, D., Toro-Escobar, C.M., Halverson, M., Skoglund, T.W. (1998b). Alluvial fans formed by channelized fluvial and sheet flow. II: Applications. *J. Hydraulic Eng.* 124(10), 996–1004.

Parker, G., Wilcock, P., Paola, C., Dietrich, W.E., Pitlick, J. (2007). Physical basis for quasi-universal relations describing bankfull hydraulic geometry of single-thread gravel bed rivers. *J. Geophys. Res. Earth* 112(F4), 21.

Parker, G., Muto, T., Akamatsu, Y., Dietrich, W.E., Lauer, J.W. (2008). Unraveling the conundrum of river response to rising sea level: From laboratory to field. Part II. The Fly-Strickland River system, Papua New Guinea. *Sedimentology* 55(6), 1657–1688.

Parker, G., Shimizu, Y., Wilkerson, G.V., Eke, E., Abad, J.D., Lauer, J.W., Paola, C., Dietrich, W.E., Voller, V.R. (2011). A new framework for modeling the migration of meandering rivers. *Earth Surf. Proc. Land* 36, 70–86.

Recking A. (2009). Theoretical development on the effects of changing flow hydraulics on incipient bedload motion. *Water Resour. Res.* 45, W04401, 16. doi:10.1029/2008WR006826

Rijn, L.C. (1984). Sediment transport, part II: Suspended load transport. *J. Hydraulic Eng.* 110(11), 1613–1641.

Soar, P.J., Thorne, C.R. (2001). Channel restoration design for meandering rivers. *Report*, ERDC/CHL CR-01-1, 416, Coastal Hydraulics Laboratory, U.S. Army Corps of Engineers, Engineer Research and Development Center.

Wilkerson, G.V., Parker, G. (2011). Physical basis for quasi-universal relationships describing bankfull hydraulic geometry of sand-bed rivers. *J. Hydraulic Eng.* **7**(1), 739–753.

Wright, S., Parker, G. (2005a). Modeling downstream fining in sand-bed rivers. I: Formulation. *J. Hydraulic Res.* 43(6), 612–619.

Wright, S., Parker, G. (2005b). Modeling downstream fining in sand-bed rivers. II: Application. *J. Hydraulic Res.* 43(6), 620–630.